AIP Journal of Applied Physics

The role of Nb in intensity increase of Er ion upconversion luminescence in zirconia

K. Smits, A. Sarakovskis, L. Grigorjeva, D. Millers, and J. Grabis

Citation: Journal of Applied Physics **115**, 213520 (2014); doi: 10.1063/1.4882262
View online: http://dx.doi.org/10.1063/1.4882262
View Table of Contents: http://scitation.aip.org/content/aip/journal/jap/115/21?ver=pdfcov
Published by the AIP Publishing

The role of Nb in intensity increase of Er ion upconversion luminescence in zirconia

K. Smits,[1,a)] A. Sarakovskis,[1] L. Grigorjeva,[1] D. Millers,[1] and J. Grabis[2]
[1]*Institute of Solid State Physics, University of Latvia, 8 Kengaraga Str., Riga LV1063, Latvia*
[2]*Institute of Inorganic Chemistry, Riga Technical University, Salaspils-1 LV2169, Latvia*

(Received 21 February 2014; accepted 28 May 2014; published online 6 June 2014)

It is found that Nb co-doping increases the luminescence and upconversion luminescence intensity in rare earth doped zirconia. Er and Yb-doped nanocrystalline samples with or without Nb co-doping were prepared by sol-gel method and thermally annealed to check for the impact of phase transition on luminescence properties. Phase composition and grain sizes were examined by X-ray diffraction; the morphology was checked by scanning- and high-resolution transmission electron microscopes. Both steady-state and time-resolved luminescence were studied. Comparison of samples with different oxygen vacancy concentrations and different Nb concentrations confirmed the known assumption that oxygen vacancies are the main agents for tetragonal or cubic phase stabilization. The oxygen vacancies quench the upconversion luminescence; however, they also prevent agglomeration of rare-earth ions and/or displacement of rare-earth ions to grain surfaces. It is found that co-doping with Nb ions significantly (>20 times) increases upconversion luminescence intensity. Hence, ZrO_2:Er:Yb:Nb nanocrystals may show promise for upconversion applications. [http://dx.doi.org/10.1063/1.4882262]

I. INTRODUCTION

Zirconia is one of the most promising oxides to be used as a host material for upconversion luminescence. This expectation is based on its high chemical and physical stability and, most importantly, on the relatively low phonon energy ($\sim$470 cm^{-1}), compared to other oxides, which is necessary for the overall efficiency of the upconversion processes in a material.[1] Zirconia is also biocompatible and non-toxic,[2,3] and it is shown that zirconia could be used for oxygen sensing.[4] Since upconversion luminescence can be utilized for temperature measurement,[5,6] the application of ZrO_2 in biology for labeling and biosensors would be attractive, if the upconversion luminescence in ZrO_2 could be significantly increased.

ZrO_2 has three polymorphs—monoclinic, tetragonal, and cubic. Only the monoclinic phase of the undoped ZrO_2 is stable at room temperature (RT); the tetragonal and cubic phases are not. It is known that the incorporation of divalent or trivalent cationic species such as Mg^{2+}, Ca^{2+}, Y^{3+} stabilize the tetragonal and/or cubic phase of ZrO_2 at RT.[7] These cationic species substitute for Zr^{4+}, and the charge compensation is provided by oxygen vacancies. Rare earth (RE) ions in zirconia are mostly trivalent, they substitute for Zr^{4+} ions and, thus, stabilize the tetragonal or cubic phase.

Tetravalent RE ions appear only at high doping concentrations.[8] EXAFS analysis shows that in tetragonal and cubic phases, the oxygen vacancies are associated mostly with the Zr in the vicinity of the RE ion rather than directly with the dopant ion.[9,10] The dielectric measurements performed on the doped zirconia have shown similar results.[11] Thus, the surrounding of Zr^{4+} ion in the vicinity of the dopant is distorted, and this could affect the luminescence of RE ions.

In theoretical studies, oxygen vacancies were suggested to be the main cause for tetragonal and cubic structure stabilization.[12] Thus, it is believed that the stabilization of phase by different dopants is not due to the difference in ionic radii, but rather due to lattice relaxation caused by oxygen vacancies.

The local distortion results in a preferential increase of the O 2p(π)–Zr 4d(e_g) covalent bonding. This would contribute to the tetragonal or cubic phase stabilization force.[8] However, the phase stabilization of zirconia is a more complex process: apart from lattice relaxation around oxygen vacancies, the collective effects between cations are also involved.[13]

Phase transition in pure zirconia under irradiation was observed by Simeone *et al.*[14] They proposed that trapping of electrons at oxygen vacancies (F-center formation) could affect the lattice relaxation and cause phase transition. The existence of F-type centers in yttrium stabilized zirconia single crystals was verified by transient absorption measurements.[15]

The grain size of zirconia nanocrystals determines the phase of the undoped material. For grain sizes below 30 nm, the tetragonal phase is stable at RT due to the excess surface energy.[16]

The luminescence of RE ion-doped ZrO_2 has been studied by a number of researchers. RE ion luminescence characteristics in zirconia are concentration-dependent, however, the concentration quenching in zirconia nanocrystals is present only at relatively high concentrations, which indicates that the RE distribution in nanocrystals is homogeneous.[17] The spectral distribution of RE ion luminescence depends on the ZrO_2 grain size, because of the change of local crystal field around the RE ion.[18–20] On one hand, the increase in grain size reduces the concentration of surface defects, thus decreasing the rate of nonradiative recombination's. On the other hand, the increase of the grain size at activator concentrations less then 3 mol. %

a)E-mail: smits@cfi.lu.lv

can lead to monoclinic phase formation. In this case, at higher temperatures, the RE ions can be squeezed out to the grain surfaces and/or agglomerate.[21]

For the upconversion luminescence centre, we chose Er ion, however, other RE species such as Sm, Tm, and Tb could be used as well.[22–24] The doping with Yb enhances the efficiency of upconversion process due to the large optical absorption cross-section of Yb ion for pumping at $\sim 1\,\mu m$ and effective energy transfer (ET) to Er ions.[23,25] Additionally, Yb doping of zirconia nanocrystals increases the intensity of the red luminescence of Er.[26] Both Er and Yb incorporate in Zr^{4+} sites as RE^{3+}; therefore, oxygen vacancies are required to compensate the charge. It was assumed by Fabris *et al.*[12] that oxygen vacancies stabilize the tetragonal or even cubic zirconia phase. It was also shown by Wang *et al.*[27] that Er doping greatly increases the luminescence of intrinsic defects, indicating the increase of their concentration. This luminescence is related to oxygen vacancies and can be varied by changing oxygen vacancy concentration in zirconia nanocrystals.[28] Oxygen vacancies suppress the upconversion luminescence.[21] Therefore, in order to increase the RE ion luminescence and upconversion luminescence in zirconia, the concentration of oxygen vacancies must be reduced.

The addition of Nb^{5+} not only reduces oxygen vacancies[29,30] but also affects the phase of zirconia.[31,32] However, the Nb-doped zirconia has been studied only for ionic conductivity applications.

The energy transfer involved in upconversion luminescence in Er and Yb co-doped zirconia could be dependent both on oxygen vacancy concentration and on zirconia phase. Therefore, an additional doping with Nb^{5+}, as well as different annealing of ZrO_2:Er:Yb nanocrystals was carried out in the present study, and the luminescence of the samples was examined. In this report, we show that the additional doping with Nb^{5+} reduces the concentration of oxygen vacancies necessary for RE^{3+} charge compensation, while the annealing of the material changes the grain sizes as well as the phase of zirconia.

II. MATERIALS AND METHODS

A. Zirconia nanoparticle samples

Er- and Yb-doped zirconia nanoparticles $ZrO_2(0.97\text{-}x)$, $Er_2O_3(0.01)$, $Yb_2O_3(0.02)$, $Nb_2O_5(X)$ were obtained with various Nb_2O_5 concentrations using sol-gel method.[33,34]

All chemicals used were reagent grade, supplied by Aldrich. The samples were prepared using zirconium chloride—99.9% ($ZrCl_4$—CAS 1026-11-6), erbium oxide—99.99% (Er_2O_3—CAS 12061-16-4), ytterbium oxide—99.99% (Yb_2O_3—CAS 1314-37-0), niobium chloride—99.8% ($NbCl_5$—CAS 1026-12-7), methanol (CH_3OH—CAS 67-56-1), nitric acid—65% (HNO_3—CAS 697-37-2), glycine ($C_2H_5NO_2$—CAS 56-40-6), and deionized water as precursors.

$ZrCl_4$ and $NbCl_5$ were dissolved in methanol. The appropriate amounts of Er_2O_3, Yb_2O_3, and Nb_2O_5 were dissolved in an excess of nitric acid. The molar concentration of all metal ions in the solution was adjusted to 0.2M with deionized water. Chloride ions were eliminated with a nitric acid excess. After stirring for 20–30 min, a glycine solution was added. The molar ratio of metal ions and glycine was 1:2, and the molar ratio of glycine/NO_3^- was 0.7.

The appropriate amounts of metal solutions and glycine were mixed, and the resulting mixture was then evaporated on a hot plate while stirring at 90–100 °C and concentrated until a gel consistence was obtained. The gel was heated to 300–350 °C in an open oven for 2 h to promote combustion to eliminate the nitric oxide. The final product was a black powder. After annealing at temperatures over 700 °C, the powder turned to white.

Six samples with different Nb concentration (0, 0.3, 1.5, 3, 6, and 12 mol. % Nb_2O_5) and with fixed 1 mol. % Er_2O_3 and 2 mol. % Yb_2O_3 concentration were synthesized (Table I). The samples obtained were split into four parts and annealed for 2 h at different temperatures (800, 1000, 1200, and 1400 °C).

To verify the impact of oxygen vacancies on luminescence of samples 1 and 4 (without Nb_2O_5 and with 3 mol. %, respectively), these samples were additionally annealed in nitrogen atmosphere at 800 °C for 1 h.

Phase composition of the prepared samples was determined by X-ray diffraction analysis (XRD) (D8 Advance, Bruker AXS). The crystallite size was calculated from the broadening of the diffraction peaks using DIFFRAC plus BASIC Evaluation Package (EVA) Release 2007 (Bruker AXS) software. The crystallite size verification and morphology studies were made using SEM Lyra (Tescan) operated at 25 kV and TEM Tecnai G20 (FEI) operated at 200 kV. The samples for TEM studies were supported by carbon coated grid; for SEM, the samples were attached to a conductive adhesive carbon tape and coated with gold.

The energy-dispersive X-ray analysis of the samples was performed using Eagle III XPL (EDAX) and S4 Pioneer

TABLE I. Dopant concentrations in samples, determined form synthesis data (left column) and measured by XRF fundamental parameters method on two different spectrometers.

	Synthesis (mol. %)			XRF 1 (mol. %)			XRF 2 (mol. %)		
Sample	Er_2O_3	Yb_2O_3	Nb_2O_5	Er_2O_3	Yb_2O_3	Nb_2O_5	Er_2O_3	Yb_2O_3	Nb_2O_5
1	1	2	0	1.82	3.54	0	0.64	1.8	0
2	1	2	0.3	1.6	3.27	0.38	0.62	1.72	0.17
3	1	2	1.5	1.7	3.3	1.54	0.65	1.73	1.24
4	1	2	3	1.73	3.13	2.99	0.64	1.75	2.48
5	1	2	6	1.77	3.2	5.59	0.63	1.7	4.94
6	1	2	12	1.78	3.44	11.49	0.64	1.73	10

TABLE II. Phase compositions and crystallite sizes determined by XRD analysis. Phase abbreviations: M-monoclinic, T-tetragonal, and N-niobates.

	XRD				Crystallite size (XRD) (nm)			
Sample	800 °C	1000 °C	1200 °C	1400 °C	800 °C	1000 °C	1200 °C	1400 °C
1	T	T	T	T	21	44	57	73
2	T	T	T	T	20	43	65	70
3	T	T	T + M	M + T	18	41	57	42
4	T	T + M	M	M	17	45	54	80
5	T	T + M	M + T + N	M + T + N	17	41	53	82
6	T	T + M + N	M + T + N	M + T + N	20	40	50	75

(Bruker AXS) in order to examine the Er, Yb, and Nb concentrations and to verify the absence of impurities.

B. Luminescence measurements

For luminescence measurements, the powders of ZrO_2 nanocrystals were lightly pressed into small uniformly sized stainless steel cells. This enabled a quantitative comparison of the luminescence intensities.

The steady state luminescence spectra were obtained, using five different excitation sources:(I) X-ray tube with W anode, operated at 30 kV, 10 mA, (II) 975 nm Thorlabs laser diode L975P1WJ (power 1 W) driven by Thorlabs ITC4005 controller, (III) ArF laser PSX-100-2 operating at 6.42 eV; (IV) 4th harmonic (4.66 eV) of diode-pumped YAG:Nd. For time-resolved luminescence and luminescence excitation spectra measurements the Ekspla NT342/3UV Ti-sapphire laser coupled with an optical parametric oscillator (OPO) was used. The luminescence spectra were recorded using the Andor Shamrock B-303i monochromator/spectrograph equipped with a CCD camera (Andor DU-401 A-BV). The same spectrometer equipped with PMT (H8259-02) was used for time resolved measurements of the luminescence.

III. RESULTS AND DISCUSSION

A. Morphology and structure of the nanocrystals

Six samples with different Nb concentrations (0, 0.3, 1.5, 3, 6, and 12 mol. % Nb_2O_5) and with fixed 1 mol. % Er_2O_3 and 2 mol. % Yb_2O_3 concentrations were synthesized (Table I). The concentration of the dopants was examined by two different X-ray fluorescence (XRF) spectrometers. Due to calibration problems the absolute concentration of erbium and ytterbium could not be determined. Nevertheless, it could be verified that the relative concentration of RE species remained almost constant while the Nb concentration varied.

The structure and size of nanocrystals affect luminescence[21,35] therefore, all samples were annealed at different temperatures. The structure and grain sizes were also determined for all samples. With the increase of the annealing temperature, the grain size increased (Table II).

The calculated crystallite sizes did not show any dependence on Nb concentration.

The SEM (Figure 1) and TEM (Figure 2) images show that the particles form agglomerates. The particles could be single crystals and also polycrystals (Figure 3). The most efficient crystal formation appears in temperature region close to 1200 °C, where cation diffusion takes place.

TEM images indicate that the grain size of the samples annealed at 800 °C is close to that calculated from the XRD data. However, the actual crystallite size should be smaller, since the grains seem to consist of several crystallites (Figure 3). For the samples annealed at higher temperatures, the size of particles observed in TEM micrographs (Figure 4) is two or three times larger than that calculated from XRD data.

SEM images reveal that the morphology and formation of agglomerates slightly differ with an increase of Nb doping (Figures 2 and 5). This could be related to differences in surfaces caused by different modes of charge compensation.

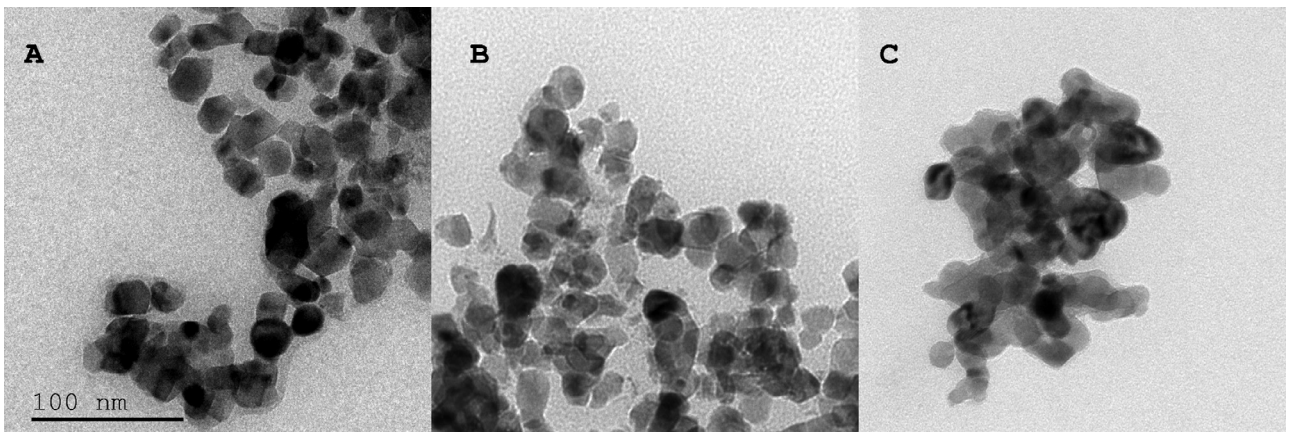

FIG. 1. TEM images for Er:Yb-doped zirconia with different Nb content: Nb-free zirconia (a), 3 mol. % (b) and 12 mol. % (c). All samples were annealed at 800 °C.

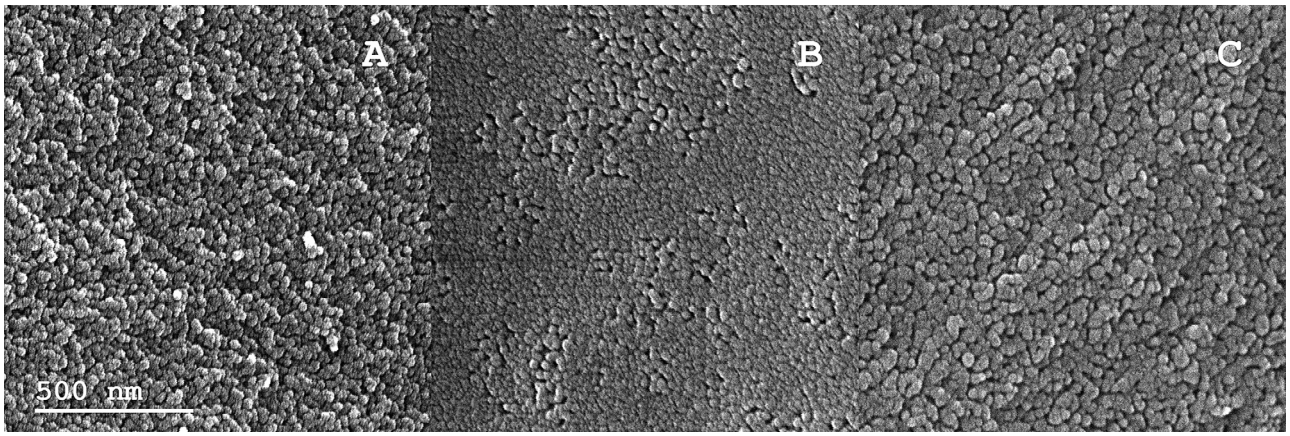

FIG. 2. SEM images for Er:Yb-doped zirconia with different Nb content: Nb-free zirconia (a), 3 mol. % (b) and 12 mol. % (c). All samples were annealed at 800 °C.

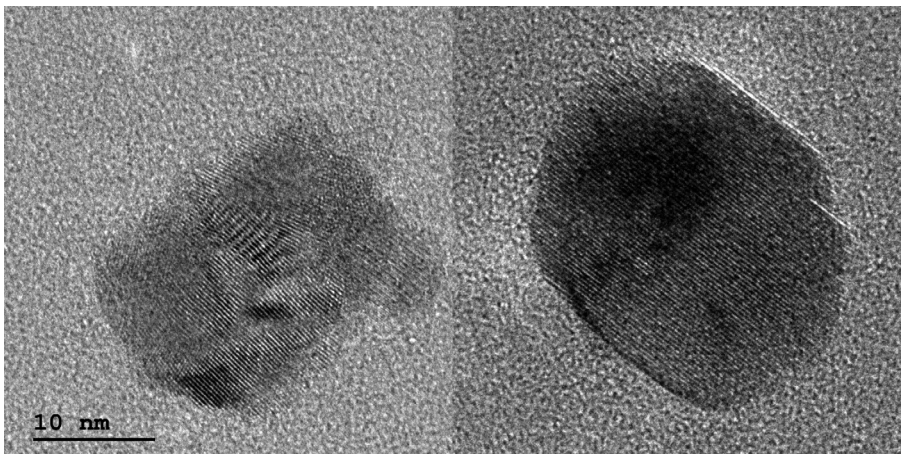

FIG. 3. TEM images of two different grains of Nb-free zirconia (sample 1) annealed at 800 °C.

The annealing of the undoped zirconia nanocrystals leads to an increase in grain size and for sizes above 30 nm; the phase transition from tetragonal to monoclinic occurs.[16] In our case of ZrO_2:Er,Yb samples, not doped by Nb, the grain size could be larger or the tetragonal/cubic phase could be fully stable at RT, due to the contribution of RE ions to tetragonal phase stabilization.

XRD patterns of Nb-free sample (Sample 1) show that the tetragonal phase is stable (Figure 6); only small traces of monoclinic phase reflection peaks could be found for the sample annealed at 1400 °C (75 nm). The doping by 1.5 mol. % of Nb_2O_5 (Sample 3) leads to the appearance of monoclinic phase at 1200 °C. The monoclinic phase becomes dominant at 1400 °C, and only 5% of the tetragonal phase is left. In the case when the Nb content is the same as the concentration of RE dopants (Sample 4), the monoclinic phase appears at 1000 °C, and the sample turns fully monoclinic after annealing at the temperatures above 1200 °C.

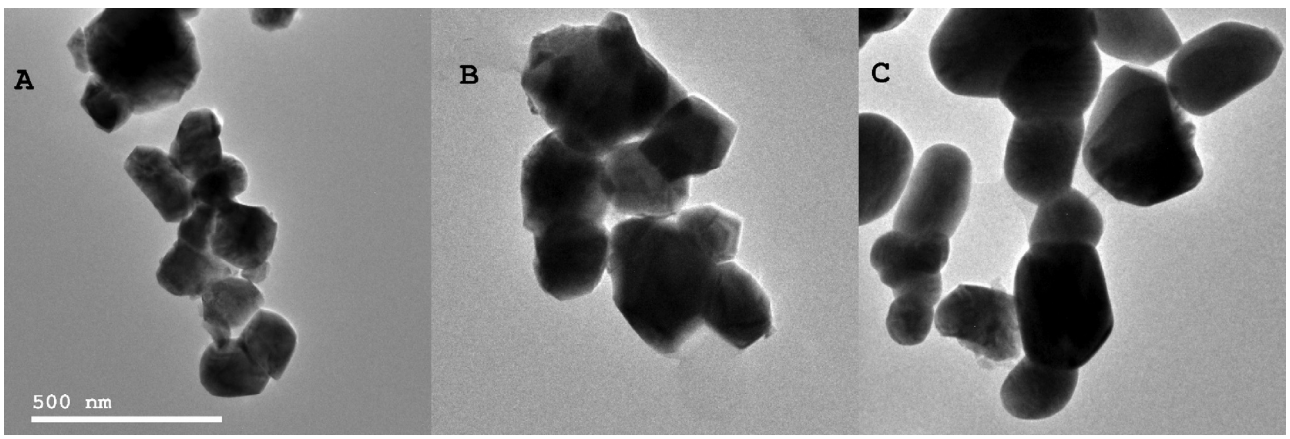

FIG. 4. TEM images for Er:Yb-doped zirconia with different Nb content: Nb-free zirconia (a), 3 mol. % (b) and 12 mol. % (c)). All samples were annealed at 1000 °C.

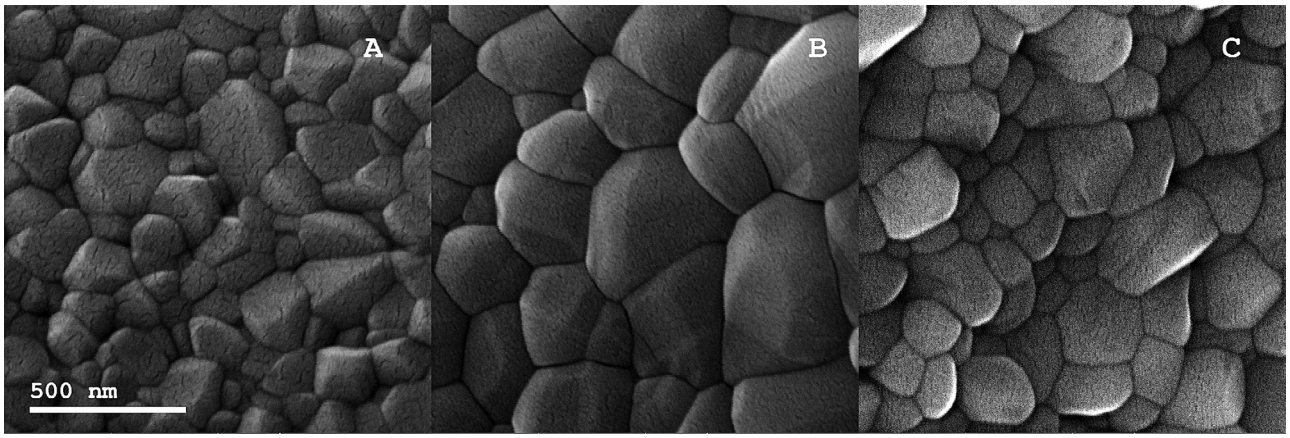

FIG. 5. SEM images for Er:Yb-doped zirconia with different Nb content: Nb-free zirconia (a), 3 mol. % (b) and 12 mol. % (c)). All samples were annealed at 1000 °C.

When the sample is doped with RE ions, for every two RE ions, one oxygen vacancy for charge compensation is required. In the cases when not only RE^{3+} but also niobium ions are introduced into zirconia, for each trivalent RE ion, one Nb^{5+} can compensate the charge difference. In this case, no oxygen vacancies are needed, and therefore, the phase transition to monoclinic phase occurs. This result is in agreement with the suggestion that the main species responsible for zirconia tetragonal phase stabilization are oxygen vacancies.

The further increase in Nb concentration (Samples 5 and 6) leads to the formation of niobates or niobium zirconates, for example, $Nb_2Zr_6O_{17}$ (temperatures 1200 °C and 1400 °C). The sample description, doping concentrations, and estimated crystal phases are shown in Table II.

B. Luminescence measurements

Erbium ions in zirconia can be excited in four processes: (I) direct excitation of Er^{3+} (single photon or multi-photon excitation for upconversion luminescence); (II) excitation of Er-O ligand (the charge transfer could be involved); (III) excitation of zirconia matrix over band gap ($E \sim 5$–5.5 eV[36]) followed by energy transfer to Er^{3+}; (IV) in up-conversion process involving the energy transfer from Yb^{3+} to Er^{3+}. Therefore, for understanding of the Nb impact on Er luminescence, we studied erbium luminescence using different excitation sources. In Er- and Yb-doped ZrO_2 nanocrystals, Nb-codoping strongly increases the intensity of upconversion luminescence (Figure 7) compared to the samples without Nb. Since the main upconversion mechanism in Yb-Er doped systems is energy transfer from Yb^{3+} to Er^{3+}, it appears that in Nb doped samples, the efficiency of energy transfer process between the RE ions is more efficient. This suggests that oxygen vacancies in Nb undoped samples suppress the energy transfer. The annealing temperature also increases the intensity of upconversion luminescence, which could be explained by the grain growth and defect redistribution. When Nb doped samples are annealed at temperatures above 1000 °C, the integral intensity of upconversion luminescence (area 540–550 nm) increases up to twenty times compared to the samples without Nb (Figure 8(a)). The highest intensity of upconversion luminescence is for the sample annealed at 1200 °C, for the sample annealed at 1400 °C, this intensity is lower despite the larger grain size.

The quenching of upconversion luminescence in Er- and Yb-doped zirconia and titania samples annealed at high temperatures was described earlier.[21,37,38] High annealing temperatures and prolonging of the annealing times at these temperatures led to the quenching of upconversion luminescence.[33,39] The cation diffusion in tetragonal Ce and Yb-doped zirconia was noticed at 1200 °C; however, the anion diffusion is six orders of magnitude faster.[40] Thus, both the anions and cations are mobile above 1200 °C and redistribution of dopants could be expected. Therefore, the decrease of upconversion luminescence intensity for the samples annealed above 1200 °C could be explained by agglomeration of the RE ions and their redistribution closer to grain surfaces.

Annealing above 800 °C also changes the spectral distribution of upconversion luminescence in the Nb-doped samples (Figure 9(b)). For the samples without Nb (Sample 1), regardless of the annealing temperature, the shapes of the spectra are almost the same (Figure 9(a)). Only oxygen ions are mobile below 1200 °C, therefore the variation of spectral distribution in Nb-doped sample can be related to the changes in oxygen sublattice. The samples without Nb have almost the same luminescence spectral distribution as the samples annealed at different temperatures, because (i) the tetragonal phase is stable, (ii) oxygen vacancies are uniformly distributed over the lattice, and (iii) the surrounding environment of RE ions does not change. The increase in annealing temperature leads to a change in the surroundings of RE ions in Nb-doped zirconia. This is mainly due to phase transition from tetragonal to monoclinic. At the same time, the upconversion luminescence intensity increases. This increase can not be explained by the appearance of the monoclinic phase, because in the samples without Nb and with low Er and Yb content (insufficient for tetragonal phase stabilization) upconversion luminescence strongly decreases, when tetragonal to monoclinic phase transition occurs.[21] This indicates that it is mainly the presence of oxygen vacancies, which suppress the upconversion luminescence, regardless of the phase of zirconia.

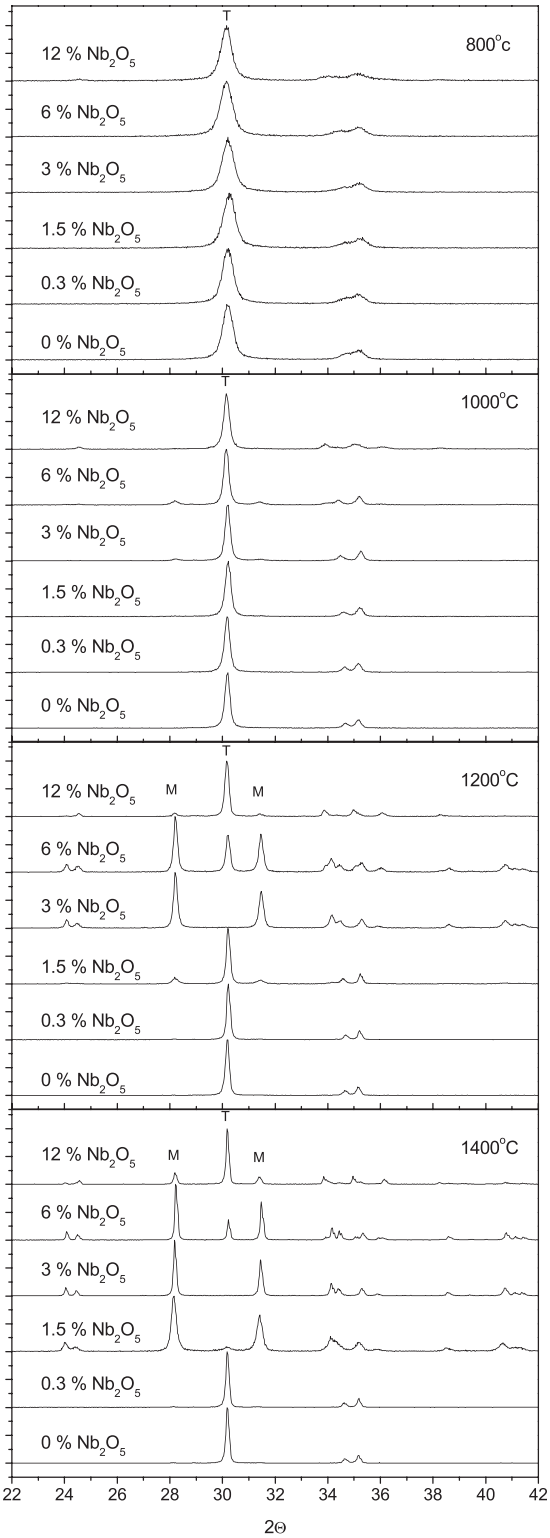

FIG. 6. X-ray diffraction patterns for ZrO_2:Er:Yb samples with different Nb contents annealed at four selected temperatures. The reflex peaks corresponding to the main monoclinic phase are indicated by M and by T for the tetragonal phase.

The variations of luminescence spectral distribution between the samples suggest that the excitation spectra of the luminescence could be different too. Therefore, to ensure clarity and to avoid the possibility that only a fraction of RE ions in a specific surrounding/phase has been excited under the 975 nm excitation used so far, we measured the upconversion luminescence excitation spectra (Figure 10); the integral luminescence was detected within 540–550 nm range. The excitation spectra for the Nb-doped and Nb-free samples differ. However, the luminescence intensities are much higher for Nb-doped samples in all excitation spectra, which confirms that upconversion process is more effective in Nb-doped samples.

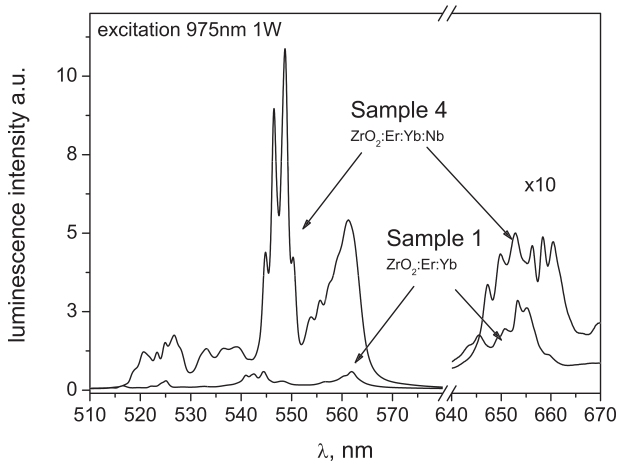

FIG. 7. Upconversion luminescence for Er:Yb-doped zirconia with 3 mol. % additional doping by Nb (Sample 4) and for Nb-free zirconia (Sample 1). Both samples have been annealed at 1000 °C.

There are three mechanisms by which green and red upconversion luminescence in Er- and Yb-doped materials can be excited. The first mechanism is a simple Er^{3+} ion excited state absorption (ESA), where Yb^{3+} are not involved. The second mechanism is energy transfer upconversion (ETU) between two erbium ions, which initially are both in the excited state ($^4I_{11/2}$). After the ETU process one of the ions is de-excited to $^4I_{15/2}$ state, whereas the other is excited to $^4F_{7/2}$ state. Finally, the third mechanism of the upconversion process is ET from Yb^{3+} ($^2F_{5/2}$) to Er^{3+} ($^4I_{11/2}$).[41] Additional information about these upconversion luminescence mechanisms can be gained the luminescence kinetics, both from its rise and decay parts. The upconversion luminescence kinetics for the sample heavily doped with Nb is similar to that for the sample without Nb. In contrast, the luminescence decay strongly differs for the sample having the same Nb content as the total content of RE ions (Figure 11). Moreover, the initial stage of the slow component has a rising part of about 4 μs. These decay components represent several upconversion processes possible in Yb^{3+}, Er^{3+}&unknown_hyphen;doped systems. The luminescence decay in all samples can not be approximated by a single exponent, it is more complicated and consists of at least two components. It could be well fitted by two exponents. The fast components of the decay for the samples 1, 4, and 6 are 12.9, 20.5, and 13.1 μs while the slow components −25.5, 94.7, and 38.8 μs, respectively. The fast component of the decay kinetics is related to ESA mechanism occurring in a single Er^{3+} ion as sequential photon absorption ($^4I_{15/2} \rightarrow {}^4I_{11/2}$, $^4I_{11/2} \rightarrow {}^4F_{7/2}$). The slow part of luminescence decay kinetics also includes the Energy Transfer process between Er^{3+} ions ($^4I_{11/2}$, $^4I_{11/2} \rightarrow {}^4I_{15/2}$, $^4F_{7/2}$) or Energy Transfer between Yb^{3+} and Er^{3+} ([Yb^{3+}] $^2F_{5/2} \rightarrow {}^2F_{7/2}$, [$Er^{3+}$]$^4I_{15/2} \rightarrow {}^4I_{11/2}$), ([$Yb^{3+}$] $^2F_{5/2} \rightarrow {}^2F_{7/2}$, [$Er^{3+}$]$^4I_{11/2} \rightarrow {}^4F_{7/2}$). The slow component of

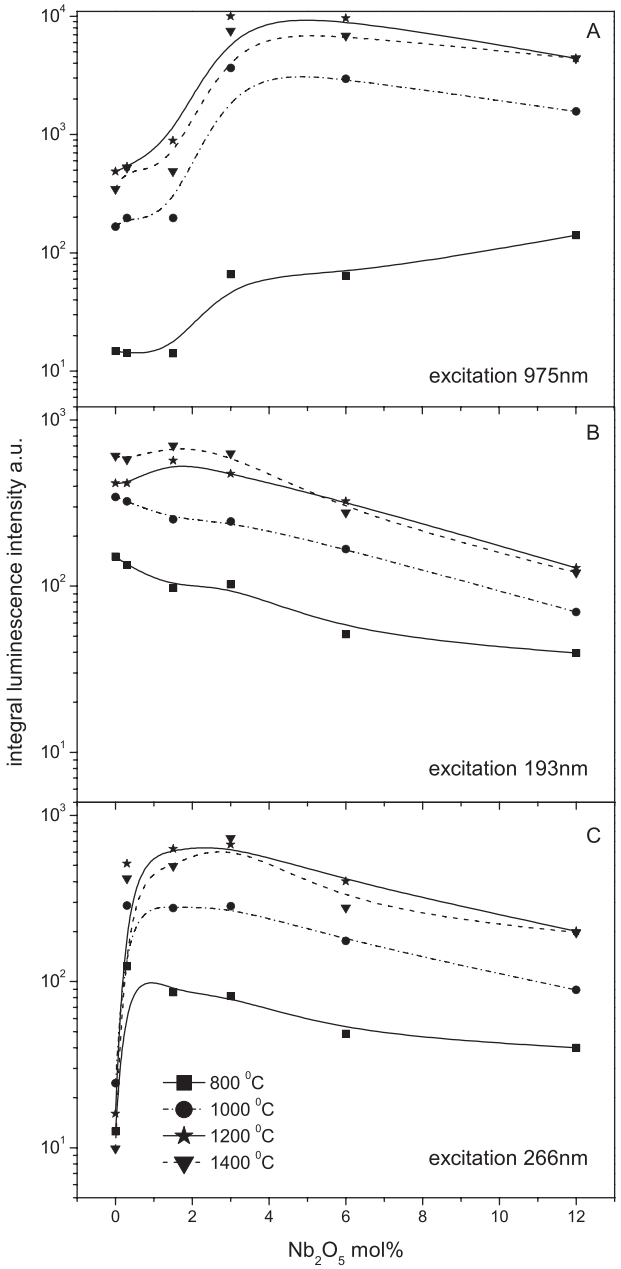

FIG. 8. Integral intensity of the luminescence as a function of Nb content in the samples used in this study.

the upconversion luminescence is well-pronounced for the sample with Nb signifying the higher probability of ET in this sample. In the sample without Nb, the slow component is considerably less pronounced, which might be explained by the presence of oxygen vacancies in the sample that disturb the ET between the RE ions.

To study further the impact of Nb on Er luminescence, we excited zirconia matrix, with the ArF 193 nm laser. For sample 1, the intensity of Er luminescence increases with the increase of the annealing temperature (Figure 8(b)). Additional doping by Nb decreases the intensity of the main Er luminescence bands for the samples annealed below 1000 °C, whereas for the samples annealed above 1000 °C, the intensity of the luminescence increases and reaches maximum for Nb concentration of 1.5 mol. %. Further increase of Nb concentration leads to decrease of the intensity. The

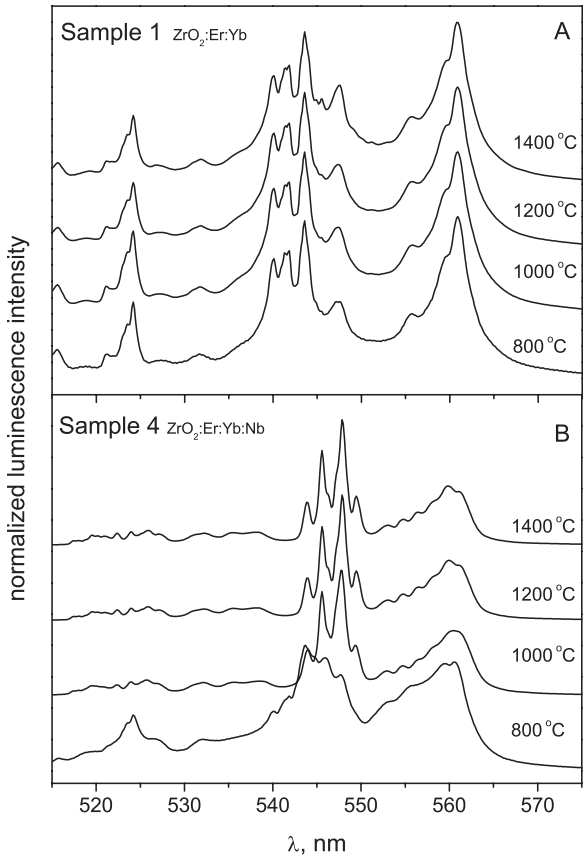

FIG. 9. Dependence of the upconversion luminescence intensity on annealing temperature in Nb-free sample (a) and in sample doped by 3 mol. % Nb (b).

down-conversion luminescence is a first order process; therefore, the luminescence intensity is not so strongly affected by oxygen vacancies as in the upconversion case; however, the spectrum of the down-conversion luminescence is similar to that observed for the upconversion luminescence (Figure 12).

The concentration of oxygen vacancies is smaller in samples of Nb-doped ZrO_2:Er,Yb, therefore, the energy transfer is more efficient and the intensity of the upconversion luminescence is improved. However, it is possible that the Nb^{5+}

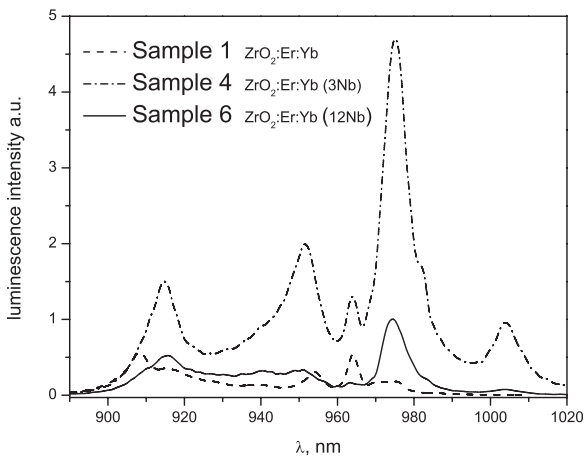

FIG. 10. Upconversion luminescence excitation spectra for Er:Yb-doped zirconia samples with different Nb content: Nb-free zirconia (Sample 1), 3 mol. % (Sample 4) and 12 mol. % (Sample 6). All samples were annealed at 1000 °C.

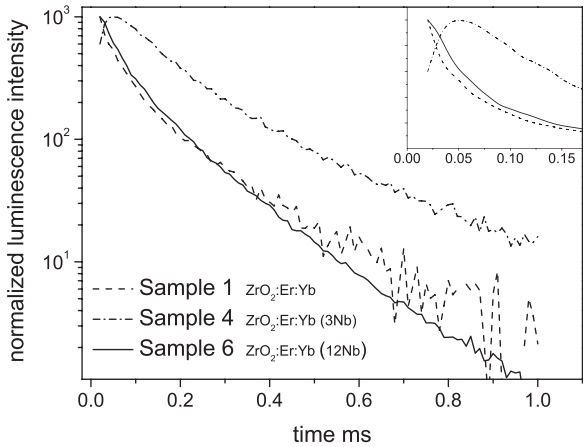

FIG. 11. Upconversion luminescence decay kinetics excited at 972 nm for Er:Yb-doped zirconia samples with different Nb content: Nb-free zirconia (Sample 1), 3 mol. % (Sample 4), and 12 mol. % (Sample 6). All samples were annealed at 1200 °C. The inset graph shows the initial part of luminescence decay.

directly contributes to the transfer processes. This possibility is supported by an observation of a very intense Er^{3+} luminescence under 266 nm excitation in the Nb-doped sample, whereas only a trace of Er^{3+} luminescence could be detected (about hundred times lower) in Nb-free sample (Figure 8(c)). Additionally, the optical absorption spectra of Samples 1 and 4 are different (Figure 13). The absorption band in niobates was observed at 290 nm.[42] This corresponds to the absorption edge shift when the Nb is added. It is possible that in ZrO_2:Er,Yb,Nb, a photoexcitation in this spectral region leads to the charge transfer from oxygen surrounding of Nb^{5+}. One could expect that the RE^{3+} ion interacts with both the niobium and its surrounding oxygen ions, and charge transfer in this complex leads to the formation of RE^{3+} excited state. Therefore, excitation at 266 nm results in a very efficient RE^{3+} luminescence. This result could also indicate that RE^{3+} and Nb^{5+} ions incorporated in zirconia are in a close proximity. Optical absorption spectrum (Figure 13) for Nb-free sample shows larger absorption within 300–900 nm region compared to Nb- doped sample indicating that number of intrinsic defects in Nb-free sample is higher.

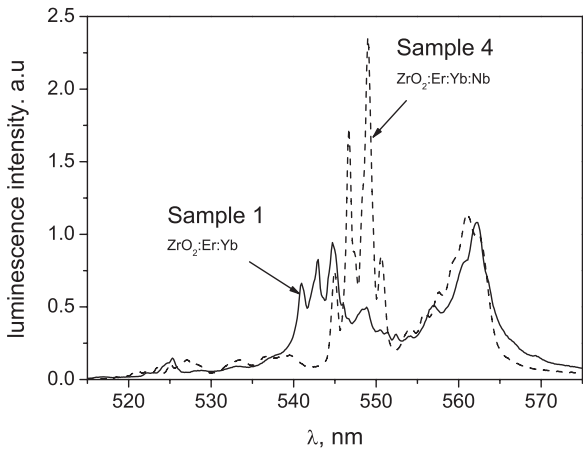

FIG. 12. Luminescence for Er:Yb-doped zirconia with 3 mol. % additional doping by Nb (Sample 4) and for Nb-free zirconia (Sample 1) excited over band gap (193 nm). Both samples have been annealed at 1000 °C.

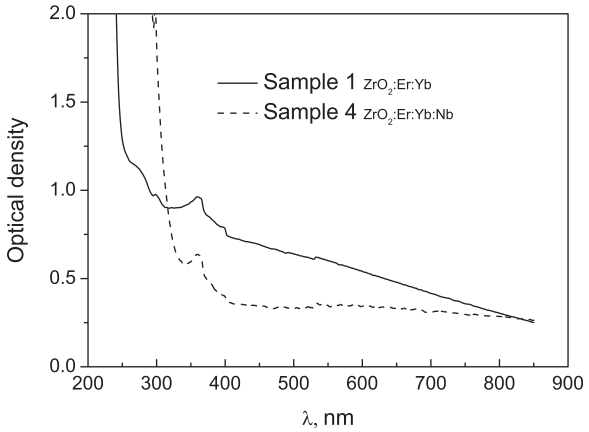

FIG. 13. Absorption spectra of Er:Yb-doped zirconia with 3 mol. % additional doping by Nb (Sample 4) and for Nb-free zirconia (Sample 1). Both samples have been annealed at 1000 °C.

Regardless of the excitation source, a consistent pattern can be observed for the Er^{3+} luminescence bands in the 540–550 nm region. The Er^{3+} bands are more intense in the 545–550 nm region for Nb-codoped samples and around 540 nm in Nb-free ones. These spectral distribution differences are expected to be due to the presence of oxygen vacancies. Previous studies show that it is possible to introduce additional oxygen vacancies in zirconia.[2,21,28,43] The annealing of the samples with and without Nb in a nitrogen atmosphere leads to a strong quenching of upconversion luminescence. However, for the Nb-free sample, luminescence reduction is three times stronger compared to the Nb-doped sample (Sample 4). This reduction is related to the number of oxygen vacancies in zirconia; in Nb-free samples, these vacancies are favorable, and for local charge compensation are located close to RE^{3+} ions. For the Nb-doped samples, the increase of oxygen vacancy concentration is less favorable, since the role of charge compensator is taken by Nb ion. The spectral distribution of the upconversion luminescence for the Sample 1 changes due to the annealing, whereas for the Sample 4, the spectral distribution before and after the annealing in nitrogen is almost the same. The relative decrease of Er ion luminescence in Nb-free sample is the strongest in the 545–550 nm region, which is exactly the same spectral region where the Er ion luminescence is the strongest in samples with Nb (Figure 14). All Er ion spectral lines are present in both Nb-doped and Nb-free samples, indicating that Nb directly does not change the surroundings of Er ion. Therefore, the dominant Er luminescence bands at 541 and 542.5 nm could be related to luminescence originating from Er adjacent to oxygen vacancy, whereas the bands at 547 nm and 549 nm—to Er ions in surroundings without oxygen vacancies. However, the luminescence properties of RE-O-Zr-O-RE complexes and the role of oxygen vacancies in the energy transfer processes require additional research.

In fluorides, the optimal Er and Yb concentrations for efficient upconversion luminescence are significantly larger[44] than used in the present study. Therefore, it is expected that for ZrO_2:Er,Yb,Nb, the optimal Er and Yb concentration could be significantly larger as well.

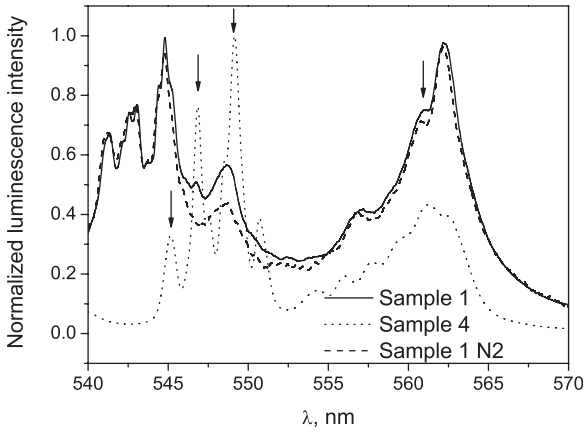

FIG. 14. Upconversion luminescence measured for Er:Yb-doped zirconia with 3 mol. % additional doping by Nb (Sample 4) and for Nb-free zirconia (Sample 1), where Sample 1 N2 was additionally annealed in nitrogen atmosphere at 900 °C.

IV. CONCLUSIONS

The Nb doping increases the efficiency of photoluminescence, especially the upconversion luminescence, of Er- and Yb-doped ZrO_2 nanocrystals, thus making zirconia more attractive for luminophore applications. We have shown the impact of oxygen vacancies and RE ion distribution in the material on luminescence quenching. Both the concentration of oxygen vacancies and the RE distribution are determined by charge compensation necessary for incorporation of RE^{3+} ions in Zr^{4+} sites.

We have also shown that the addition of Nb increases the probability of phase transition from tetragonal to monoclinic. Our experiments confirm the previous results based on theoretical modeling, which indicate that oxygen vacancies are the main agents for tetragonal-cubic phase stabilization in zirconia.

We assume that such charge compensation model in zirconia and the effect on luminescence intensity are valid for the most of the RE ions.

ACKNOWLEDGMENTS

This work was supported by the Latvian Science Council Grant No. 2013.10-5/014 (LZP N 302/2012) The authors are grateful to Aija Krumina and Linards Skuja for XRF and XRD analysis.

[1]N. Maeda, N. Wada, H. Onoda, A. Maegawa, and K. Kojima, Thin Solid Films **445**, 382 (2003).
[2]J. Chevalier, Biomaterials **27**, 535 (2006).
[3]K. Smits, J. Liepins, M. Gavare, A. Patmalnieks, A. Gruduls, and D. Jankovica, IOP Conf. Ser.: Mater. Sci. Eng. **38**, 012050 (2012).
[4]T. Chudoba, K. Galazka, L. Grigorjeva, W, Łojkowski, D. Millers, A. Opalinska, K. Smits, and A. Swiderska-Sroda, WO 2012110967 (EP2686669A1) A1 (23.8.2012).
[5]Y. Shen, X. Wang, H. He, Y. Lin, and C. W. Nan, J. Alloys Compd. **536**, 161 (2012).
[6]M. M. Gentleman and D. R. Clarke, Surf. Coat. Technol. **188-189**, 93 (2004).
[7]R. C. Garvie, J. Phy. Chem. **82**, 218 (1978).
[8]J. Yuan, T. Hirayama, Y. Ikuhara, and T. Sakuma, Micron **30**, 141 (1999).
[9]B. W. Veal, A. G. McKale, A. P. Paulikas, S. J. Rothman, and L. J. Nowicki, Physica B **150**, 234 (1988).
[10]M. Cole, C. R. Catlows, and J. P. Dragu, Phys. Chem. Solids **51**, 507 (1990).
[11]M. Kurumada, H. Hara, and E. Iguchi, Acta Mater. **53**, 4839 (2005).
[12]S. Fabris, A. T. Paxton, and M. W. Finnis, Acta Mater. **50**, 5171 (2002).
[13]P. Villella, S. D. Conradson, F. J. Espinosa-Faller, S. R. Foltyn, K. E. Sickafus, and J. A. Valdez, Phys. Rev. B **64**, 104101 (2001).
[14]D. Simeone, G. Baldinozzi, D. Gosset, and S. Le Caer, Nucl. Instrum. Methods Phys. Res., Sect. B **250**, 95 (2006).
[15]K. Smits, L. Grigorjeva, D. Millers, J. D. Fidelus, and W. Lojkowski, IEEE Trans. Nucl. Sci. **55**, 1523 (2008).
[16]R. C. Garvie, J. Phys. Chem. **69**, 1238 (1965).
[17]K. Smits, L. Grigorjeva, D. Millers, A. Sarakovskis, A. Opalinska, J. D. Fidelus, and W. Lojkowski, Opt. Mater. **32**, 827 (2010).
[18]L. Huangqing, W. Lingling, C. Shuguang, Z. Bingsuo, and P. Zhiwei, Appl. Surf. Sci. **253**, 3872 (2007).
[19]S. Lange, I. Sildos, M. Hartmanova, V. Kiisk, E. E. Lomonova, and M. Kirm, J. Phys.: Conf. Ser. **249**, 012007 (2010).
[20]C.-G. Ma, M. G. Brik, V. Kiisk, T. Kangur, and I. Sildos, J. Alloys Compd. **509**, 3441 (2011).
[21]K. Smits, D. Jankovica, A. Sarakovskis, and D. Millers, Opt. Mater. **35**, 462 (2013).
[22]S. Lange, I. Sildos, M. Hartmanova, J. Aarik, and V. Kiisk, J. Non-Cryst. Solids **354**, 4380 (2008).
[23]D. Solis, E. De la Rosa, O. Meza, L. A. Diaz-Torres, P. Salas, and C. A. Chavez, J. Appl. Phys. **108**, 023103 (2010).
[24]M. R. N. Soares, C. Nico, J. Rodrigues, M. Peres, M. J. Soares, A. J. S. Fernandes, F. M. Costa, and T. Monteiro, Mater. Lett. **65**, 1979 (2011).
[25]F. Vetrone, J. C. Boyer, J. A. Capobianco, A. Speghini, and M. Bettinelli, J. Appl. Phys. **96**, 661 (2004).
[26]L. A. Gomez, L. de S. Menezes, C. B. de Araujo, R. R. Goncalves, S. J. L. Ribeiro, and Y. Messaddeq, J. Appl. Phys. **107**, 113508 (2010).
[27]X. Wang, J. Zhao, P. Du, L. Guo, X. Xu, and C. Tang, Mater. Res. Bull. **47**, 3916 (2012).
[28]K. Smits, L. Grigorjeva, D. Millers, A. Sarakovskis, J. Grabis, and W. Lojkowski, J. Lumin. **131**, 2058 (2011).
[29]X. Guo and Z. Wang, J. Eur. Ceram. Soc. **18**, 237 (1998).
[30]Z. Wang, Z. Q. Chen, J. Zhu, S. J. Wang, and X. Guo, Radiat. Phys. Chem. **58**, 697 (2000).
[31]D. J. Kim, J. Am. Ceram. Soc. **73**, 115 (1990).
[32]D. J. Kim, H. J. Jung, and D. H. Cho, Solid State Ionics **80**, 67 (1995).
[33]D. G. Lamas, G. E. Lascelea, and N. E. Walsoe de Reca, J. Eur. Ceram. Soc. **18**, 1217 (1998).
[34]K. A. Singh, L. C. Pathak, and S. K. Roy, Ceram. Int. **33**, 1463 (2007).
[35]T. Lopez- Luke, E. De la Rosa, D. Solis, P. Salas, C. Angeles-Chavez, A. Montoya, L. A. Diaz-Torres, and S. Bribiesca, Opt. Mater. **29**, 31 (2006).
[36]N. G. Petrik, D. P. Taylor, and T. M. Orlando, J. Appl. Phys. **85**, 6770 (1999).
[37]D. E. Harrison, N. T. McLamed, and E. C. Subarao, J. Electrochem. Soc. **110**, 23 (1963).
[38]J. Zhang, X. Wang, W. T. Zheng, X. G. Kong, Y. J. Sun, and X. Wang, Mater. Lett. **61**, 1658 (2007).
[39]D. Solis, T. Lopez-Luke, E. De la Rosa, P. Salas, and C. Angeles-Chavez, J. Lumin. **129**, 449 (2009).
[40]J. Thornton, A. Majumdar, and G. MacAdams, Surf. Coat. Technol. **94–95**, 112 (1997).
[41]A. Patra, C. S. Friend, R. Kapoor, and P. N. Prasad, J. Phys. Chem. B **106**, 1909 (2002).
[42]Y. Zhou, Z. Qiu, M. Lu, A. Zhang, and Q. Ma, J. Lumin. **128**, 1369 (2008).
[43]K. Smits, L. Grigorjeva, W. Lojkowski, and J. D. Fidelus, Phys. Status Solid **4**, 770 (2007).
[44]N. Menyuk, K. Dwight, and J. W. Pierce, Appl. Phys. Lett. **21**(4), 159 (1972).